Title

Direct Observation of the Transition-State Region in the Photodissociation of CH3I by Femtosecond Extreme Ultraviolet Transient Absorption Spectroscopy

Journal

The Journal of Physical Chemistry Letters, 6(24)

ISSN

1948-7185

Authors

Attar, Andrew R
Bhattacherjee, Aditi
Leone, Stephen R

Publication Date

2015-12-17

DOI

10.1021/acs.jpclett.5b02489

Peer reviewed

THE JOURNAL OF PHYSICAL CHEMISTRY Letters

Letter

pubs.acs.org/JPCL

Direct Observation of the Transition-State Region in the Photodissociation of CH_3I by Femtosecond Extreme Ultraviolet Transient Absorption Spectroscopy

Andrew R. Attar,[†,‡] Aditi Bhattacherjee,[†,‡] and Stephen R. Leone*[,†,‡,§]

[†]Department of Chemistry, University of California, Berkeley, California 94720, United States

[‡]Chemical Sciences Division, Lawrence Berkeley National Laboratory, Berkeley, California 94720, United States

[§]Department of Physics, University of California, Berkeley, California 94720, United States

Supporting Information

ABSTRACT: Femtosecond extreme ultraviolet (XUV) pulses produced by high harmonic generation are used to probe the transition-state region in the 266 nm photodissociation of CH_3I by the real-time evolution of core-to-valence transitions near the iodine N-edge at 45−60 eV. During C−I bond breaking, new core-to-valence electronic states appear in the spectra, which decay concomitantly with the rise of the atomic iodine resonances of $I(^2P_{3/2})$ and $I^*(^2P_{1/2})$. The short-lived features are assigned to repulsive valence-excited transition-state regions of $^3Q_0$ and $^1Q_1$, which can connect to transient core-excited states via promotion of 4d(I) core electrons. A simplified one-electron transition picture is described that accurately predicts the relative energies of the transient states observed. The transition-state resonances reach a maximum at ∼40 fs and decay to complete C−I dissociation in ∼90 fs, representing the shortest-lived chemical transition state observed by core-level, XUV, or X-ray spectroscopy.

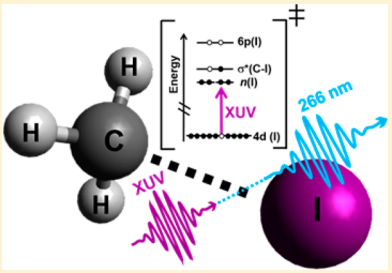

Extreme ultraviolet (XUV)/X-ray absorption spectroscopy is an exceptionally powerful method for probing the electronic structure of molecules through the fingerprint of core-to-valence transitions. Steady-state XUV and X-ray absorption measurements provide remarkable sensitivity to the oxidation states, spin-states, chemical environment, and electronic structure of long-lived reactants and products.[1−4] However, a key to understanding chemical reaction dynamics is in the characterization of the transition-state region *between* the thermodynamic minima of reactants and products.[5] With the development of methods for generating ultrashort X-ray pulses using high-harmonic generation (HHG), X-ray slicing, and free electron lasers (FELs), the uniquely powerful capabilities of core-to-valence spectroscopies are now being applied in the ultrafast time domain to study short-lived states and species, and even to gain unprecedented access to the electronic structure of transition states of chemical reactions.[4,6−15] While other spectroscopic methods have enabled the detection and temporal tracing of transition states in the recent past,[5,16−19] the frontier of femtosecond X-ray techniques is now aiming to exploit its particular advantages to reveal detailed, atom-specific chemical information regarding the bonding and valence electronic structure in the transition-state region. In the present work, we apply femtosecond XUV transient absorption spectroscopy based on a HHG source to directly observe the evolving valence electronic structure in the transition-state region of the sub-100 fs photodissociation reaction of methyl iodide in the A band. This is the shortest-lived molecular transition state captured by core-level, X-ray or XUV spectroscopy. Furthermore, the evidence for a direct observation of the evolving valence electronic structure through the chemical transition-state region is particularly clear.

The UV absorption spectrum of methyl iodide in the A-band is characterized by $n(I) \rightarrow \sigma^*(C-I)$ transitions corresponding to promotion of a nonbonding electron localized on the iodine atom to an antibonding orbital localized on the C−I bond.[20] The optically allowed states include two weak perpendicular transitions to the $^3Q_1$ and $^1Q_1$ states and one strong parallel transition to the $^3Q_0$ state.[20−23] A-band decomposition reveals that 266 nm absorption is characterized essentially entirely by the $^3Q_0$ state, correlating to the spin−orbit excited I atom ($^2P_{1/2}$), or I*.[24] There is a conical intersection near the Franck−Condon window for absorption, allowing crossing onto the $^1Q_1$ surface, which is correlated to the ground-state I atom ($^2P_{3/2}$).[25] Dissociation to I* via the $^3Q_0$ state is the major reaction channel at 266 nm by a ratio of ∼3:1.[26,27] Femtosecond clocking measurements that probe the rise of the final atomic products have determined dissociation times for I and I* channels of 84 ± 12 fs and 94 ± 6 fs, respectively.[28] Here, we utilize 4d(I) core-to-valence transitions to follow the dissociation process *through* the $^3Q_0$ and $^1Q_1$ transition-state regions and to the final atomic products.

The UV-pump, XUV-probe experimental apparatus, and methodology have been previously described[12] and are

Received: November 6, 2015
Accepted: December 4, 2015
Published: December 4, 2015

DOI: 10.1021/acs.jpclett.5b02489
J. Phys. Chem. Lett. 2015, 6, 5072−5077

discussed in detail in the Supporting Information. Briefly, gas-phase CH_3I molecules are photoexcited into the A band via one-photon absorption at 266 nm. The photoexcited molecules are probed with broadband (35−60 eV, sub-35 fs) XUV pulses, which are produced via HHG driven by two-color 800 nm (1.6 mJ) + 400 nm (25 μJ) driving pulses in Ar gas. The transient absorption spectra (ΔOD) are obtained by measuring the energy-resolved XUV transmission through the sample in the presence of the 266 nm pump pulse, at a particular pump−probe time delay, relative to the XUV transmission in the absence of the pump pulse, $\Delta OD = -\log(I_{on}/I_{off})$.

The probing scheme is qualitatively presented in Figure 1a from the perspective of the potential energy curves along the C−I reaction coordinate and in Figure 1b−e from the molecular orbital perspective, showing the relevant orbitals. Transient core-to-valence resonances of the dissociating molecule are observed for the first time, which represent the evolution of the valence electronic structure from the transition-state region to the products. The observations can be understood in terms of a simple one-electron transition picture, wherein the 4d core electrons are promoted to fill the "optical hole" in the n(I) valence orbital following 266 nm excitation.

The ground-state electronic configuration of methyl iodide in C_{3v} symmetry is $\cdots(\mathbf{4d})^{10}(1a_1)^2(2a_1)^2(1e)^4(3a_1)^2(\mathbf{2e})^4(\mathbf{4a_1})^0$. The relevant orbitals in bold include the 4d(I) core orbitals; the 2e nonbonding orbitals on the iodine atom, which represent the highest occupied molecular orbital (HOMO); and the $4a_1$ orbital, which is the σ^*(C−I) lowest unoccupied molecular orbital (LUMO). In Figure 2, the static, ground-state XUV absorption spectrum of methyl iodide is shown, and the result is an excellent match to the spectrum previously obtained using a synchrotron source.[29] The resonant pre-edge transitions are labeled A−F and overlap with an underlying, nonresonant absorption due to valence and core-level ionization. The assignments of the resonances are shown in Table 1.[29] A spin−orbit doublet is observed for each final state electron configuration, characterized by the ∼1.7 eV spin−orbit splitting of the $(4d_{5/2})^{-1}$ and the $(4d_{3/2})^{-1}$ states with an I(4d) core-hole.[29−31] The most prominent doublet, with resonances at 50.6 and 52.3 eV, corresponds to promotion of a 4d(I) core electron to the σ^* (C−I) molecular orbital, resulting in a core-excited final state with an electron configuration of $\cdots(\mathbf{4d})^9(1a_1)^2(2a_1)^2(1e)^4(3a_1)^2(\mathbf{2e})^4(\mathbf{4a_1})^1$, as depicted in Figure 1b.

The 266 nm excitation in the A band of methyl iodide leads to direct dissociation of the C−I bond, forming a methyl radical and an I($^2P_{3/2}$) or I*($^2P_{1/2}$) atom. Figure 3 shows a representative data set (out of >50 data sets) of the differential absorption in the "long delay time" limit, capturing the transient absorption spectrum of the asymptotic products after photodissociation of methyl iodide. The transient absorption spectrum in Figure 3 is a time-averaged spectrum taken by summing the results of 28 time delays ranging from 300 fs to 1.5 ps. The sharp product absorption features at 46.2, 46.9, and 47.9 eV correspond to the well-known 4d → 5p core-to-valence transitions of atomic I and I* (Figure 1a). In order of ascending energy, these transitions are known to be the $^2P_{3/2}$ → $^2D_{5/2}$, $^2P_{1/2}$ → $^2D_{3/2}$, and $^2P_{3/2}$ → $^2D_{3/2}$ transitions of atomic iodine, respectively.[32,33]

To capture the dissociating molecule in the transition-state region, transient spectra at short time delays between 0 and 100 fs are compared to the final spectrum obtained from long delay

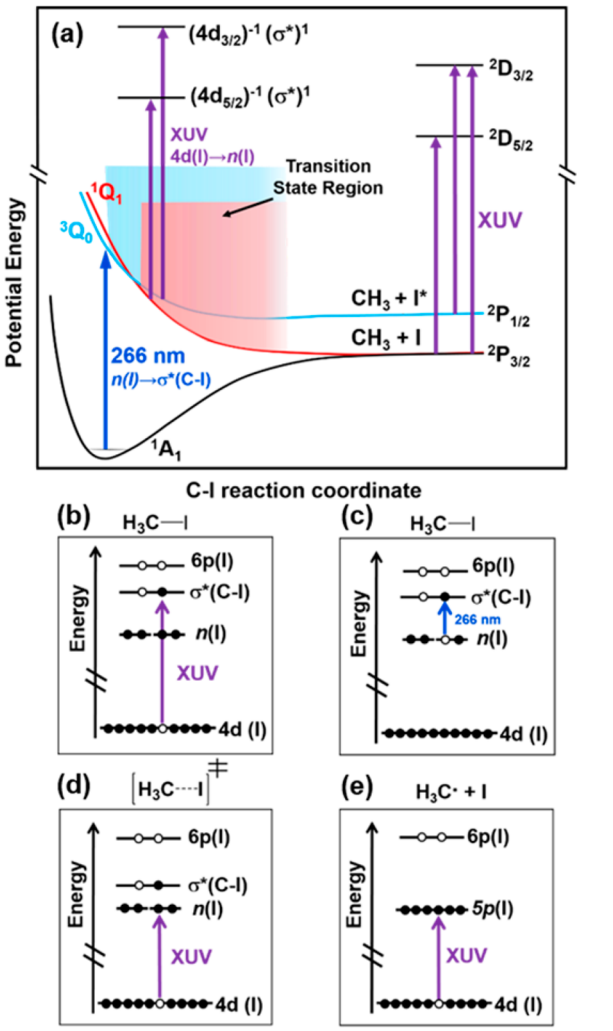

Figure 1. (a) Schematic representation showing the relevant potential energy curves along the C−I reaction coordinate with the XUV probing scheme. A 266 nm photon excites CH_3I into the $^3Q_0$ potential energy surface, which correlates with CH_3 + I*($^2P_{1/2}$) fragments. A nonadiabatic curve crossing at a conical intersection leads to population of the $^1Q_1$ state, which correlates with CH_3 + I($^2P_{3/2}$) products. While in the repulsive transition-state regions of the $^3Q_0$ and $^1Q_1$ valence-excited states, XUV absorption into transient core-excited states are represented with purple arrows. Transitions from the atomic $^2P_{3/2}$ and $^2P_{1/2}$ states into the $^2D_{5/2}$ and $^2D_{3/2}$ core-excited atomic states are drawn with purple arrows in the asymptotic limit. The $^2P_{3/2}$−$^2P_{1/2}$ and $^2D_{5/2}$−$^2D_{3/2}$ spin−orbit splittings of atomic iodine are 0.95 and 1.7 eV, respectively. (b−e) Schematic orbital diagrams showing the *final state* electron configurations accessed via (b) XUV absorption from the ground state of methyl iodide, (c) 266 nm absorption from the ground state of methyl iodide, (d) XUV absorption from the valence-excited transition-state regions of the $^3Q_0$ and $^1Q_1$ surfaces, and (e) XUV absorption from the $^2P_{3/2}$ and $^2P_{1/2}$ states of the fully separated I atom.

times of the *same* time scan. Figure 4a shows a representative example (out of six data sets) of the XUV absorption spectra near the I/I* product resonances measured during a time scan, comparing a transient spectrum captured at a time delay of 50 fs with the final product spectrum from long time delays of the same time scan. In the spectrum at 50 fs, there are clear transient features, labeled A and B, that disappear in the final spectrum at long time delays. Transient feature A appears at

DOI: 10.1021/acs.jpclett.5b02489
J. Phys. Chem. Lett. 2015, 6, 5072−5077

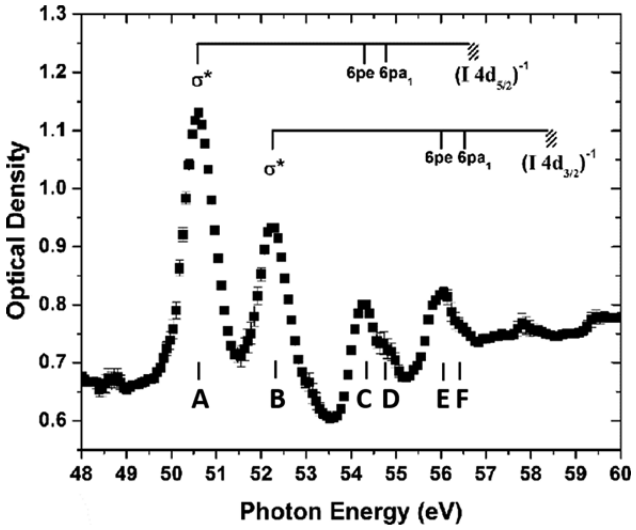

Figure 2. Static "pump off" XUV absorption spectrum of methyl iodide plotted near the I $N_{4/5}$ edge. Peaks and assignments match the high-resolution photoabsorption spectrum measured with a synchrotron source.[29] Pre-edge, core-to-valence resonances labeled A and B correspond to promotion of a 4d(I) core electron into the σ^*(C−I) orbital of the molecule. Resonances marked C−F correspond to transitions from the 4d(I) core orbital into the labeled Rydberg orbitals, which converge on the spin−orbit split $(I\ 4d_{5/2})^{-1}$ and $(I\ 4d_{3/2})^{-1}$ ionization limits.

Table 1. Static XUV Absorption, I $N_{4,5}$ Pre-edge Transition Assignments of Methyl Iodide

peak	photon energy (eV)	assignment
A	50.6	4d(I) → σ^*(C−I), $(4d_{5/2})^{-1}$
B	52.3	4d(I) → σ^*(C−I), $(4d_{3/2})^{-1}$
C	54.3	4d(I) → 6pe $(4d_{5/2})^{-1}$
D	54.8	4d(I) → 6pa_1 $(4d_{5/2})^{-1}$
E	56.0	4d(I) → 6pe $(4d_{3/2})^{-1}$
F	56.5	4d(I) → 6pa_1 $(4d_{3/2})^{-1}$

~45.6 eV as a shoulder on the low-energy side of the I atom $^2P_{3/2} \rightarrow {}^2D_{5/2}$ resonance. Transient feature B appears as a shoulder at ~47.3 eV, on the high-energy side of the I* ($^2P_{1/2} \rightarrow {}^2D_{3/2}$) resonance, and it is the more prominent of the transients. A third weaker transient feature near 48.4 eV appears at a time delay of ~50 fs in some data sets, but not in others (including the representative data set plotted in Figure 4a). Six data sets have been taken, and every data set reveals transient features A and B, but only two data sets reveal the third transient at ~48.4 eV. This third transient is apparently at the edge of the detection limit and is therefore not included in the present analysis, but it will be addressed in future work on another molecule, where it is more prominent.

In Figure 4, the temporal behaviors of the transient features A and B at short time delays are shown as lineouts of the differential absorption amplitude at 45.6 and 47.3 eV as a function of time. Because transients A and B are slightly overlapping the final product absorption, the transient absorption signals at these energies do not decay completely to zero, but rather decay to an asymptote corresponding to the small absorption amplitude in the final product spectrum (see Supporting Information). To decouple the effect of a rising product absorption that underlies the pure transient population, the background contribution from the rise of the pure atomic

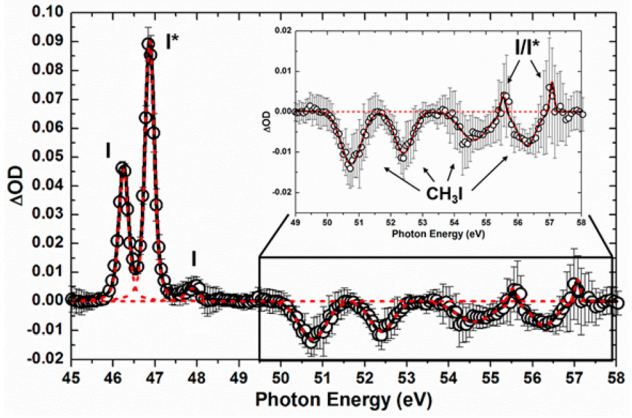

Figure 3. XUV transient absorption spectrum following completed 266 nm photodissociation of methyl iodide. Open circles are the experimental absorption data points, and the dashed red lines are Voigt functions fit to each peak. The solid black line is the sum of all the individual peak functions. Atomic 4d → 5p product resonances of I/I* appear between 46 and 48 eV.[32] Inset: magnified plot between 49 and 58 eV. The negative amplitude peaks represent the depletion of the parent molecule static absorption. There are weak 4d(I) → 6p,7p(I) product transitions of atomic iodine overlapping the molecular 4d(I) → 6p(I) depletions of the parent molecule in the energy region between 55 and 57 eV.[33]

resonances to the absorption amplitude at transients A and B is subtracted (see Supporting Information for details). The final background-subtracted lineouts of a representative data set (out of six) are plotted in Figure 4b,c. The transient features A and B rise within the temporal resolution of the experiment, peaking at ~40 fs, at which point they decay back to zero amplitude by ~90−100 fs.

The results can be interpreted based on the well-known photodissociation mechanism in the A band of methyl iodide. Immediately following the 266 nm n(I) → σ^*(C−I) valence excitation to the $^3Q_0$ state, 4d → n(I) XUV transitions from the 4d core orbital of I to the n(I) nonbonding orbital become available in the $^3Q_0$ transition-state region (Figure 1a,d). On a ~20 fs time scale,[25] a part of the wavepacket crosses onto the $^1Q_1$ surface via the conical intersection near the Franck−Condon window and XUV 4d → n(I) transitions also become available from the $^1Q_1$ transition-state region. The XUV 4d → n(I) transitions are expected to be similar in energy to the XUV 4d →5p atomic iodine transitions due to the 5pπ character of the n(I) nonbonding orbital, but may be shifted because of the interaction with the methyl fragment. As seen in Figure 4a, the transient features are close in energy to the pure atomic 4d → 5p resonances. The core-excited final states resulting from XUV 4d(I) → n(I) transitions have an electron configuration of $\cdots(\mathbf{4d})^9(1a_1)^2(2a_1)^2(1e)^4(3a_1)^2(\mathbf{2e})^4(\mathbf{4a_1})^1$ (Figure 1d), which is identical to the core-excited final states accessed via XUV 4d(I) → σ^*(C−I) transitions from the ground state (Figure 1b). There are two final states available, separated in energy by the characteristic spin−orbit splitting of the 4d core-hole, labeled in Figure 1a as $(4d_{5/2})^{-1}\sigma^*$ and $(4d_{3/2})^{-1}\sigma^*$.

To rationalize the relative energetic positions of the transient features compared with the atomic resonances to which they converge, we consider a simplified one-electron transition picture. From this picture, we can postulate that the XUV 4d → n(I) transitions should appear at energies corresponding to the difference between the 4d(I) → σ^*(C−I) transitions and the n(I) → σ^*(C−I) transitions, or in other words, the difference

DOI: 10.1021/acs.jpclett.5b02489
J. Phys. Chem. Lett. 2015, 6, 5072−5077

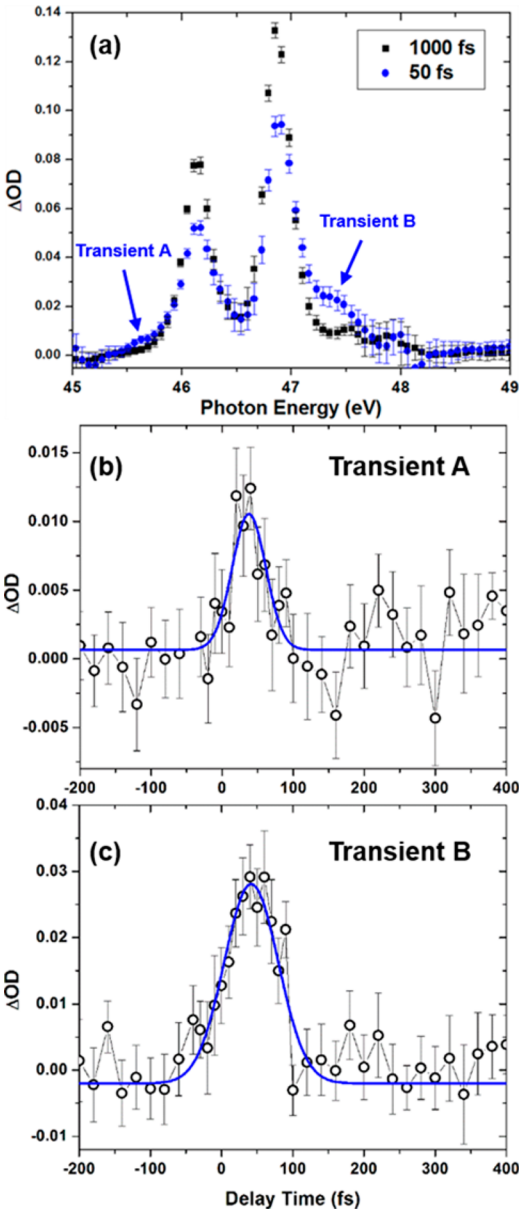

Figure 4. (a) XUV transient absorption snapshots from a representative pump−probe timescan. The transient absorption spectra at a short delay time of 50 fs (during the photodissociation reaction) and in the long delay time limit (after dissociation is fully completed) are plotted in blue circles and black squares, respectively. Transient resonances not belonging to the asymptotic products are observed during the dissociation process at ∼45.6 and ∼47.3 eV and are labeled Transient A and Transient B, respectively. (b, c) The differential absorption amplitudes at transient A (45.6 eV) and transient B (47.3 eV) are plotted as a function of pump−probe time delay in panels b and c, respectively. The open circles are the experimental absorption data points, and the blue lines are Gaussian fits. Gaussian fits are used as approximations to the convolution of the transient decays with the Gaussian instrument response function. The overlapping contribution from the asymptotic product absorption has been subtracted (see text).

in energy between the valence excited states, $^3Q_0$ and $^1Q_1$, and the core-excited states, $(4d_{5/2})^{-1}\sigma^*$ and $(4d_{3/2})^{-1}\sigma^*$. Although the potential energy surfaces of the core-excited states are not known along the dissociating C−I reaction coordinate, the energies are known at the ground-state equilibrium C−I bond length and in the asymptotic regions from the static XUV absorption spectra of CH_3I and atomic I/I*, respectively. Taking this as a starting point, the $n(I) \rightarrow \sigma^*(C-I)$ transition to the $^3Q_0$ state is 4.7 eV above the ground state, while the $(4d_{5/2})^{-1}\sigma^*$ and $(4d_{3/2})^{-1}\sigma^*$ core-excited states are found from the static absorption measurement to be 50.6 and 52.3 eV above the ground state, respectively (peaks A and B in Figure 2). Therefore, we can expect transition energies of 45.9 and 47.6 eV for the $^3Q_0 \rightarrow (4d_{5/2})^{-1}\sigma^*$ and $^3Q_0 \rightarrow (4d_{3/2})^{-1}\sigma^*$ resonances, respectively, at the equilibrium bond length. In the asymptotic region, the $^3Q_0$ state correlates with the $^2P_{1/2}$ state of atomic iodine and the upper core-excited states become $^2D_{5/2}$ and $^2D_{3/2}$. The energy differences between the $^2P_{1/2}$ state and the two atomic core-excited states are 46.9 and 45.2 eV, respectively. Although the $^2P_{1/2} \rightarrow {}^2D_{5/2}$ transition in the asymptotic region is forbidden by the dipole selection rule, the energy difference between these two states puts a lower limit on the $^3Q_0 \rightarrow (4d_{5/2})^{-1}\sigma^*$ resonance in the transition-state region. From the energetic considerations above, one can predict two possible resonances from the $^3Q_0$ transition-state region: the $^3Q_0 \rightarrow (4d_{5/2})^{-1}\sigma^*$ transition between 45.9 and 45.2 eV and the $^3Q_0 \rightarrow (4d_{3/2})^{-1}\sigma^*$ transition between 47.6 and 46.9 eV. These predicted resonance energies agree well with the observed energies of the observed transients A and B at ∼45.6 eV and ∼47.3 eV.

The same procedure can be performed for the $^1Q_1$ transition-state region, subtracting the energy of 5.2 eV[24] for the $^1Q_1$ state at the equilibrium bond length from the 50.6 and 52.3 eV energies of the $(4d_{5/2})^{-1}\sigma^*$ and $(4d_{3/2})^{-1}\sigma^*$ states and comparing to the final product resonance energies of 46.2 eV (47.9 eV) for the $^2P_{3/2} \rightarrow {}^2D_{5/2}$ ($^2P_{3/2} \rightarrow {}^2D_{3/2}$) transition in the asymptotic region. In this way, the $^1Q_1 \rightarrow (4d_{5/2})^{-1}\sigma^*$ resonance is predicted to appear in the range of 45.4−46.2 eV, and the $^1Q_1 \rightarrow (4d_{3/2})^{-1}\sigma^*$ resonance should appear between 47.1 and 47.9 eV. Again, these predicted resonance energies match well with the observed energies of transients A and B at ∼45.6 and ∼47.3 eV. Apparently, both transients A and B could arise from absorption in either or both of the $^3Q_0$ and $^1Q_1$ transition-state regions. In the present study, transients A and B appear with similar intensities in both parallel and perpendicular pump−probe polarization configurations. Based on energetics, transient A is assigned to transitions into the $(4d_{5/2})^{-1}\sigma^*$ core-excited state and transient B assigned to transitions into the $(4d_{3/2})^{-1}\sigma^*$ core-excited state, but the assignment of contributions to $^3Q_0$ and $^1Q_1$ is not yet determined. Although further calculations and experiments are needed to determine the relative contribution of each transition to the observed transient spectrum, the simple and intuitive one-electron transition picture already provides predictive power for the experimental observations without detailed calculations of the accessible states.

Previous femtosecond clocking experiments, which probe the rise of products in the asymptotic region, determined the A-band photodissociation times of methyl iodide to be 84 ± 12 fs and 94 ± 6 fs for I and I*, respectively.[28] The dynamics of the transient features A and B observed in the present studies reflect the motion of the photoexcited methyl iodide molecule through the transition-state region *before* reaching the asymptotic region. Both transient features observed here rise to a maximum at ∼40 fs and decay completely on a time scale shorter than ∼90 fs, providing the lifetimes of the transition states and connecting well to the picture of the dissociation time scales measured in the clocking experiments. Given the

DOI: 10.1021/acs.jpclett.5b02489
J. Phys. Chem. Lett. 2015, 6, 5072−5077

sub-100 fs time scale of the entire bond-breaking process, the transients still shift too fast to capture a continuous energetic shift via the spectrum, which would allow one to map more detail about the core-excited potential energy surfaces. Instead, the intensity is spread over a broader range with shifted centers of gravity relative to the pure atomic resonances, which reflects the average energy difference between valence- and core-excited states in the transition-state region compared to the asymptotic region. Nevertheless, transients A and B represent a direct observation of the evolving valence electronic structure in the localized vicinity of the I atom of methyl iodide during dissociation, exemplifying the unique capabilities of time-resolved X-ray spectroscopy to reveal detailed chemical information on transition states with atomic-site specificity. In future experiments, with even better temporal resolution (e.g., using compressed 266 nm pump pulses below 10 fs and isolated attosecond XUV probe pulses), it may be possible to fully map the core-excited state potential energy surface along the C−I reaction coordinate.

In summary, femtosecond transient core-to-valence absorption spectroscopy is used to noninvasively and directly probe the transition-state region of a prototypical photodissociation reaction. The XUV absorption spectrum captured at sub-100 fs time delays (e.g., 50 fs in Figure 4a) provides a direct observation of the transient valence electronic structure in the transition-state region leading to photoinduced bond-breaking of methyl iodide. This is the shortest-lived chemical transition state ever observed by core-level, X-ray, or XUV spectroscopy. An intuitive one-electron transition picture closely approximates the experimentally determined energies of the transient resonances. The results presented here provide a benchmark for future experiments and calculations aimed at leveraging the powerful advantages of XUV and X-ray core-to-valence absorption spectroscopy to expand our understanding of transition states of chemical reactions.

■ ASSOCIATED CONTENT

Supporting Information

The Supporting Information is available free of charge on the ACS Publications website at DOI: 10.1021/acs.jpclett.5b02489.

Experimental Methods and a description of the procedure for subtraction of background product absorption rise from transients (PDF)

■ AUTHOR INFORMATION

Corresponding Author

*E-mail: srl@berkeley.edu.

Notes

The authors declare no competing financial interest.

■ ACKNOWLEDGMENTS

This work, A.R.A., and A.B., as well as a portion of the materials and equipment were supported by the U.S. Department of Energy, Office of Science, Office of Basic Energy Sciences, under Contract DE-AC02-05CH11231, the gas phase chemical physics program through the Chemical Sciences Division of Lawrence Berkeley National Laboratory. The apparatus was partially funded by a NSF ERC, EUV Science and Technology, under a previously completed grant (EEC-0310717).

■ REFERENCES

(1) Chen, J. G. NEXAFS Investigations of Transition Metal Oxides, Nitrides, Carbides, Sulfides and Other Interstitial Compounds. *Surf. Sci. Rep.* **1997**, *30*, 1−152.

(2) de Groot, F. M. F. High Resolution X-Ray Emission and X-Ray Absorption Spectroscopy. *Chem. Rev.* **2001**, *101*, 1779−1808.

(3) Stöhr, J. *NEXAFS Spectroscopy*; Springer: Berlin, Germany, 1996.

(4) Khalil, M.; Marcus, M. A.; Smeigh, A. L.; Mccusker, J. K.; Chong, H. H. W.; Schoenlein, R. W. Picosecond X-Ray Absorption Spectroscopy of a Photoinduced Iron(II) Spin Crossover Reaction in Solution Picosecond X-Ray Absorption Spectroscopy of a Photoinduced Iron(II) Spin Crossover Reaction in Solution. *J. Phys. Chem. A* **2006**, *110*, 38−44.

(5) Polanyi, J. C.; Zewail, A. H. Direct Observation of the Transition State. *Acc. Chem. Res.* **1995**, *28*, 119−132.

(6) Gawelda, W.; Johnson, M.; de Groot, F. M. F.; Abela, R.; Bressler, C.; Chergui, M. Electronic and Molecular Structure of Photoexcited $[Ru^{II}(bpy)_3]^{2+}$ Probed by Picosecond X-Ray Absorption Spectroscopy. *J. Am. Chem. Soc.* **2006**, *128*, 5001−5009.

(7) Bressler, C.; Milne, C.; Pham, V.-T.; ElNahhas, A.; van der Veen, R. M.; Gawelda, W.; Johnson, S.; Beaud, P.; Grolimund, D.; Kaiser, M.; et al. Femtosecond XANES Study of the Light-Induced Spin Crossover Dynamics in an Iron(II) Complex. *Science* **2009**, *323*, 489−492.

(8) Huse, N.; Cho, H.; Hong, K.; Jamula, L.; de Groot, F. M. F.; Kim, T. K.; McCusker, J. K.; Schoenlein, R. W. Femtosecond Soft X-Ray Spectroscopy of Solvated Transition-Metal Complexes: Deciphering the Interplay of Electronic and Structural Dynamics. *J. Phys. Chem. Lett.* **2011**, *2*, 880−884.

(9) Vura-Weis, J.; Jiang, C.-M.; Liu, C.; Gao, H.; Lucas, J. M.; de Groot, F. M. F.; Yang, P.; Alivisatos, A. P.; Leone, S. R. Femtosecond $M_{2,3}$-Edge Spectroscopy of Transition-Metal Oxides: Photoinduced Oxidation State Change in α-Fe_2O_3. *J. Phys. Chem. Lett.* **2013**, *4*, 3667−3671.

(10) Jiang, C.-M.; Baker, L. R.; Lucas, J. M.; Vura-Weis, J.; Alivisatos, A. P.; Leone, S. R. Characterization of Photo-Induced Charge Transfer and Hot Carrier Relaxation Pathways in Spinel Cobalt Oxide (Co_3O_4). *J. Phys. Chem. C* **2014**, *118*, 22774−22784.

(11) Dell'Angela, M.; Anniyev, T.; Beye, M.; Coffee, R.; Gladh, J.; Katayama, T.; Kaya, S.; Krupin, O.; Larue, J.; Nordlund, D.; et al. Real-Time Observation of Surface Bond Breaking with an X-Ray Laser. *Science* **2013**, *339*, 1302−1305.

(12) Attar, A. R.; Piticco, L.; Leone, S. R. Core-to-Valence Spectroscopic Detection of the CH_2Br Radical and Element-Specific Femtosecond Photodissociation Dynamics of CH_2IBr. *J. Chem. Phys.* **2014**, *141*, 164308−164317.

(13) Siefermann, K. R.; Pemmaraju, C. D.; Neppl, S.; Shavorskiy, A.; Cordones, A. A.; Vura-Weis, J.; Slaughter, D. S.; Sturm, F. P.; Weise, F.; Bluhm, H.; et al. Atomic-Scale Perspective of Ultrafast Charge Transfer at a Dye-Semiconductor Interface. *J. Phys. Chem. Lett.* **2014**, *5*, 2753−2759.

(14) Canton, S. E.; Kjær, K. S.; Vankó, G.; van Driel, T. B.; Adachi, S.; Bordage, A.; Bressler, C.; Chabera, P.; Christensen, M.; Dohn, A. O.; et al. Visualizing the Non-Equilibrium Dynamics of Photoinduced Intramolecular Electron Transfer with Femtosecond X-Ray Pulses. *Nat. Commun.* **2015**, *6*, 6359−6368.

(15) Öström, H.; Öberg, H.; Xin, H.; LaRue, J.; Beye, M.; Dell'Angela, M.; Gladh, J.; Ng, M. L.; Sellberg, J. A.; Kaya, S.; et al. Probing the Transition State Region in Catalytic CO Oxidation on Ru. *Science* **2015**, *347*, 978−982.

(16) Zhong, D. P.; Cheng, P. Y.; Zewail, A. H. Bimolecular Reactions Observed by Femtosecond Detachment to Aligned Transition States: Inelastic and Reactive Dynamics. *J. Chem. Phys.* **1996**, *105*, 7864−7867.

(17) Zhong, D. P.; Zewail, A. H. Femtosecond Real-Time Probing of Reactions. 23. Studies of Temporal, Velocity, Angular, and State Dynamics from Transition States to Final Products by Femtosecond-Resolved Mass Spectrometry. *J. Phys. Chem. A* **1998**, *102*, 4031−4058.

DOI: 10.1021/acs.jpclett.5b02489
J. Phys. Chem. Lett. 2015, 6, 5072−5077

(18) Vaida, M. E.; Hindelang, P. E.; Bernhardt, T. M. Femtosecond Real-Time Probing of Transition State Dynamics in a Surface Photoreaction: Methyl Desorption from CH_3I on MgO(100). *J. Chem. Phys.* **2008**, *129*, 011105−011108.
(19) Durá, J.; de Nalda, R.; Amaral, G. A.; Bañares, L. Imaging Transient Species in the Femtosecond A-Band Photodissociation of CH_3I. *J. Chem. Phys.* **2009**, *131*, 134311−134324.
(20) Mulliken, R. S. Intensities in Molecular Electronic Spectra X. Calculations on Mixed-Halogen, Hydrogen Halide, Alkyl Halide, and Hydroxyl Spectra. *J. Chem. Phys.* **1940**, *8*, 382−395.
(21) de Nalda, R.; Izquierdo, J. G.; Durá, J.; Bañares, L. Femtosecond Multichannel Photodissociation Dynamics of CH_3I from the A-Band by Velocity Map Imaging. *J. Chem. Phys.* **2007**, *126*, 021101−021104.
(22) de Nalda, R.; Durá, J.; García-Vela, A.; Izquierdo, J. G.; González-Vázquez, J.; Bañares, L. A Detailed Experimental and Theoretical Study of the Femtosecond A-Band Photodissociation of CH_3I. *J. Chem. Phys.* **2008**, *128*, 244309−244328.
(23) García-Vela, A.; de Nalda, R.; Durá, J.; González-Vázquez, J.; Bañares, L. A 4D Wave Packet Study of the CH_3I Photodissociation in the A-Band. Comparison with Femtosecond Velocity Map Imaging Experiments. *J. Chem. Phys.* **2011**, *135*, 154306−154317.
(24) Eppink, A. T. J. B.; Parker, D. H. Methyl Iodide A-band Decomposition Study by Photofragment Velocity Imaging. *J. Chem. Phys.* **1998**, *109*, 4758−4767.
(25) Lao, K. Q.; Person, M. D.; Xayariboun, P.; Butler, L. J. Evolution of Molecular Dissociation through an Electronic Curve Crossing: Polarized Emission Spectroscopy of CH_3I at 266 nm. *J. Chem. Phys.* **1990**, *92*, 823−841.
(26) Hess, W. P.; Kohler, S. J.; Haugen, H. K.; Leone, S. R. Application of an InGaAsP Diode Laser to Probe Photodissociation Dynamics: I* Quantum Yields from N- and I-C_3F_7I and CH_3I by Laser Gain vs Absorption Spectroscopy. *J. Chem. Phys.* **1986**, *84*, 2143−2149.
(27) Riley, S. J.; Wilson, K. R. Excited Fragments from Excited Molecules - Energy Partitioning in Photodissociation of Alkyl Iodides. *Faraday Discuss. Chem. Soc.* **1972**, *53*, 132−146.
(28) Corrales, M. E.; Loriot, V.; Balerdi, G.; González-Vázquez, J.; de Nalda, R.; Bañares, L.; Zewail, A. H. Structural Dynamics Effects on the Ultrafast Chemical Bond Cleavage of a Photodissociation Reaction. *Phys. Chem. Chem. Phys.* **2014**, *16*, 8812−8818.
(29) Olney, T. N.; Cooper, G.; Brion, C. E. Quantitative Studies of the Photoabsorption (4.5−488 eV) and Photoionization (9−59.5 eV) of Methyl Iodide Using Dipole Electron Impact Techniques. *Chem. Phys.* **1998**, *232*, 211−237.
(30) O'Sullivan, G. The Absorption Spectrum of CH_3I in the Extreme VUV. *J. Phys. B: At. Mol. Phys.* **1982**, *15*, L327−L330.
(31) Comes, F. J. Inner Electron Excitation of Iodine in the Gaseous and Solid Phase. *J. Chem. Phys.* **1973**, *58*, 2230−2237.
(32) Pettini, M.; Mazzoni, M.; Tozzi, G. P. Excitation of the Inner 4d Shell of Neutral Iodine. *Phys. Lett. A* **1981**, *82*, 168−170.
(33) Nahon, L.; Morin, P. Experimental Study of Rydberg States Excited from the *d* Shell of Atomic Bromine and Iodine. *Phys. Rev. A: At., Mol., Opt. Phys.* **1992**, *45*, 2887−2893.

DOI: 10.1021/acs.jpclett.5b02489
J. Phys. Chem. Lett. 2015, 6, 5072−5077